Supporting Information: Where Do the Ions Reside in a Highly Charged Droplet?

Victor Kwan,[†] Anatoly Malevanets,[‡] and Styliani Consta[*,†]

†*Department of Chemistry, The University of Western Ontario, London N6A 5B7, Ontario, Canada*

‡*Department of Electrical and Computer Engineering, The University of Western Ontario, London N6A 5B9, Ontario, Canada*

E-mail: sconstas@uwo.ca

Phone: +1-519-6612111

Structure of pristine aqueous droplets

The structure of pristine water droplets up to 512 H_2O molecules for the five-site ST2 model, the four-site TIP4P model and the SPC/E (extended simple point charge) and that of 1000 H_2O molecules for certain water models has been examined in detail by Zakharov and co-workers.[S1,S2] The authors examined the sensitivity of the surface potential and surface tension on ST2, TIP4P, SPC/E water models. In our article we are mainly interested in the structure of the charged droplets, but we shall also discuss some of the characteristics of the pristine aqueous droplets modeled by TIP3P for the sake of completeness. We examine droplets with approximately 1000 and 6000 H_2O molecules at $T = 300$ K and $T = 350$ K. The bulk density of the TIP3P water model at 25° C and pressure 1.0 atm has been calculated[S3,S4] to be 1.002 ± 0.001 g/cm^3 but also values of 0.998 g/cm^2 have been reported depending on subtle details of the parametrization.[S5]

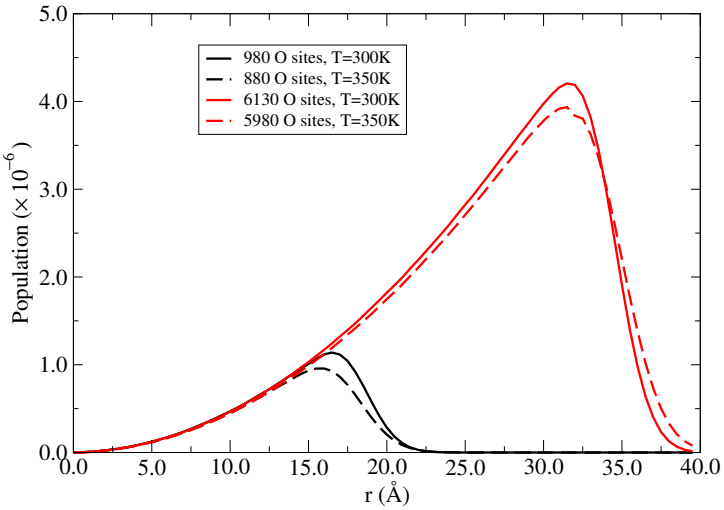

Figure S1: Raw data of the population of oxygen sites at a certain distance (r) from the droplet center of mass (COM) at $T = 300$ K (solid lines) and $T = 350$ K (dashed lines). The droplets are comprised 990 H_2O molecules and 6130 H_2O molecules at $T = 300$ K and 890 H_2O molecules and 5990 H_2O molecules at $T = 350$ K. For the histograms, we used 20000 configurations each collected every 0.2 ps and a bin size equal to 0.5 Å.

Figure S1 shows the histogram of the raw data used to prepare Fig. S2 (a). Figure S1

shows that for a droplet of 880-990 H_2O molecules the maximum population is at $r = 16.6 \pm 0.5$ Å, and overall the highest population is in the broader range of 15.5 Å $< R <$ 17.3 Å. At $r = 20.0 \pm 0.5$ Å the population decreases to 1/4 of that in the peak, thus the density reduces considerably since this population is estimated in a spherical shell of larger volume than that at $r = 16.6$ Å. The highest population is at $r = 16.6$ Å, which is > 15.9 Å, the distance at which the fast density decrease starts as shown in Fig. 2 (a) because of the larger volume available. In other words, at $r = 16.6$ Å there is the maximum population because of the volume effect, but the density has decreased earlier.

For the 6000 H_2O-molecule droplet, the maximum population is at $r = 31.5 \pm 0.5$ Å. Overall the highest population is in the broader range of 30.1 Å $< r <$ 33.0 Å. In the 6000 H_2O-molecule droplet the same density features appear as in the 1000 H_2O-molecule droplet.

Figure S2 (a) shows the density of the TIP3P H_2O molecules as a function of the distance (r) from the droplet center of mass (COM). The droplets comprised $\approx$ 1000 and $\approx$ 6000 TIP3P-H_2O molecules are found at $T = 300$ K and $T = 350$ K. Figure S2 (b) shows in colored shells the distances of the water molecules from the COM of a 6000-H_2O droplet. The water density profile (DP) shows an almost constant value up to 12.0 Å and 23.2 Å for the 1000 and 6000 H_2O-molecule droplet, respectively. At $T = 300$ K the value of the density in the core of the droplet is higher than that of the corresponding bulk solvent. As expected at 350 K, the density is lower overall than that at 300 K. At 300 K, the decrease in density is initially smooth and undergoes a faster decrease at $r \approx 15.9$ Å and $r \approx 31.2$ Å for the 1000 and 6000 H_2O-molecule droplet, respectively.

The droplet has a rough surface. In the 6000-H_2O-molecule droplet, an obvious surface roughness starts in the grey shell as shown in Fig. S2 (b). The location of the surface in a droplet has been discussed thoroughly in many surface tension studies of curved surfaces.[S6–S14] Here, we do not address the location of the surface because we think that it is not relevant to the properties we examine. In a forthcoming article we have examined the location of the surface in relation to the surface tension of highly charged droplets.

The density profiles of the pristine water droplets can be compared with those shown in Fig. 1 in Zakharov et al.[S1,S2] Calculations of Zakharov et al.[S1,S2] for clusters of 512 H_2O molecules show that the clusters at $T = 300$ K modeled by TIP4P and SPC/E have a core density very close to the bulk, but that modeled by ST2 have a higher core density than that of the bulk.

We have found that the hydrogen (H) and oxygen (O) profiles almost overlay (for clarity we do not show the hydrogen profiles). We note that there is an inversion in the order of the O and H-DP as has been found by Zakharov et al.[S1,S2] For the 6000-H_2O droplet we found that for $r < 35.35 \pm 0.5$ Å the O-DP shows a slightly higher probability density than the H-DP. The order is inverted for $r > 35.35 \pm 0.5$ Å. The change in the order of the profiles occurs smoothly. Because of this inversion, Zakharov et al.[S1,S2] consider that there is an electric double layer on the surface of water clusters.

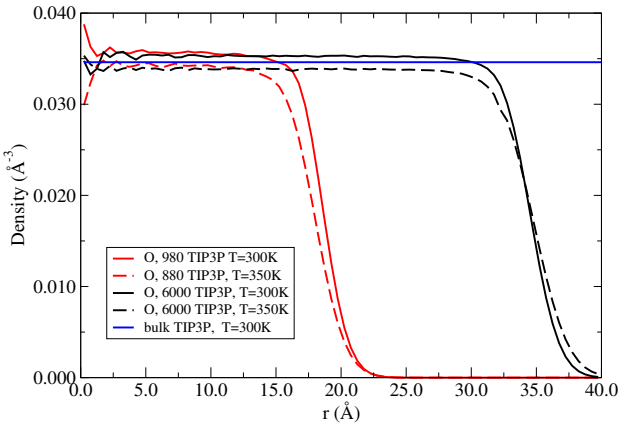

(a)

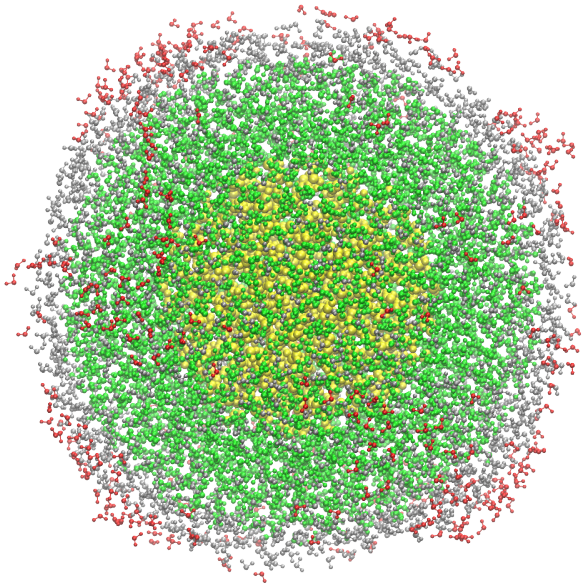

(b)

Figure S2: (a) Density of oxygen sites as a function of the distance (r) from the droplet center of mass (COM). The droplets comprised approximately 1000 and 6000 TIP3P H_2O molecules in equilibrium with its vapor at $T = 300$ K (solid lines) and $T = 350$ K (long dashed lines). The zero of the x-axis is at the droplet center of mass (COM) and the density plot starts from the center of the histogram bin, which is at 0.25 Å. The bulk density of TIP3P,[S3,S4] which is 0.03461 $\AA^{-3}$ at $T = 300$ K and pressure 1 atm is shown by the blue line. For the histograms, we used 2×10^4 configurations each collected every 0.2 ps and a bin size is 0.5 Å. Testing of smaller bin size showed the same features in the profiles. (b) Colored shells around the 6000-TIP3P droplet COM: yellow colored 0 Å $< r <$ 17.0 Å, green colored 17.0 Å $< r <$ 30.0 Å, grey colored 30.0 Å $< r <$ 34.0 Å, red colored $r >$ 34.0 Å.

Orientation of water molecules in pristine aqueous droplets

In order to examine the orientation of the electric dipoles within the droplet, we compute the distribution of $\cos(\theta)$, where θ is the angle between the H_2O dipole moment (directed from the oxygen site to the center of the line that connects the two hydrogen sites) and the vector that points from the droplet center of mass (COM) to the oxygen site of a water molecule. Both the 1000 and 6000 H_2O-molecule droplet show the same features in the angle distribution. Initially we describe the 6000 H_2O-molecule droplet.

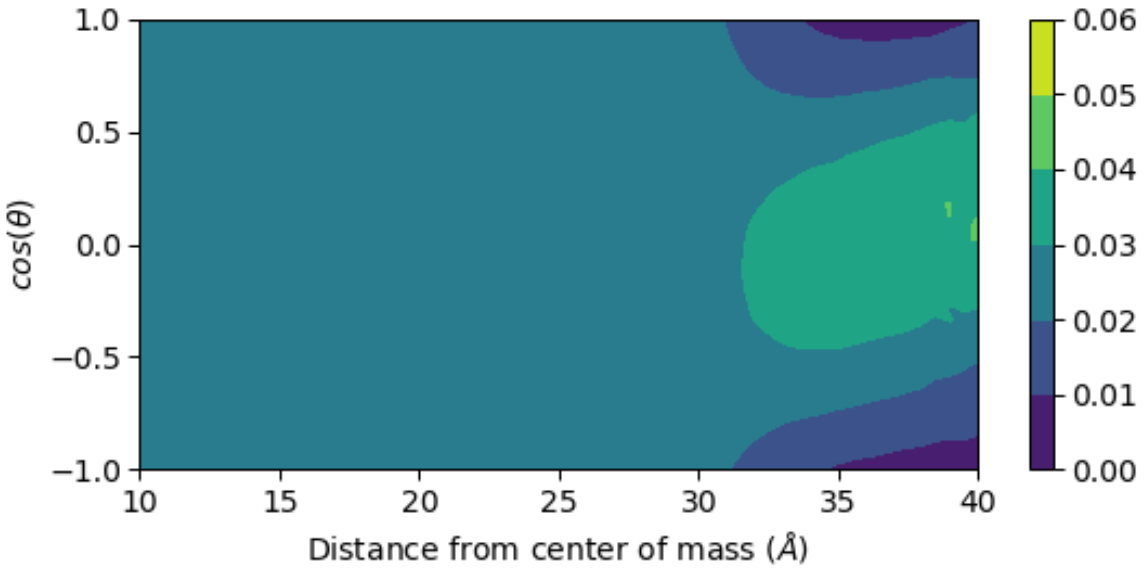

Figure S3: Contour map of $\cos(\theta)$ throughout consecutive spherical shells with center at the droplet COM for pristine aqueous droplets comprised $\approx$ 6000 TIP3P molecules at $T = 300$ K. The droplet configurations are the same as those used in Fig. S2. The bin size in $\cos(\theta)$ is 0.05 and in distance 0.5 Å.

Figure S3 shows in a contour plot the $\cos(\theta)$ distribution for a droplet of 6000 TIP3P molecules at $T = 300$ K. The $\cos(\theta)$ distributions within representative spherical shells (with center at the droplet COM and of thickness 0.5 Å) for 1000 and 6000-H_2O-molecule droplet are shown in Figs. S5 and S4. In the same figures comparison of the distributions at $T = 300$ K and $T = 350$ K is also shown. The data are normalized by dividing with the number of counts in the spherical shell.

At $r < 28$ Å the $\cos(\theta)$ distribution is uniform. The same feature has been found in other works[S1,S2] but for droplets of different size from that that we study. Thus, regardless of the size of the droplet and the water model this feature is robust. At 28 Å$< r < 35$ Å the $\cos(\theta)$ distribution is an inverted parabola (shown in Figs. S5 and S4), with a flat maximum in range $-0.25 - 0$. In approximately the same range of 28.0 Å$< r <$32.0 Å the raw data of the oxygen population is at its maximum as shown in Fig. S1. For $r >$ 32.0 Å the oxygen population decreases (Fig. S1) while the volume increases, which indicates a considerable decrease in the droplet density. At 35 Å$< r <$37 Å the $\cos(\theta)$ distribution in symmetric with respect to zero. At $r >$37 Å the $\cos(\theta)$ distribution shows a broad maximum in the range $0 - 0.25$. In the same distance ($r \approx$ 38.0 Å), the oxygen population decreases by an order of magnitude relative to that in the range 28.0 Å$< r <$32.0 Å. It is noted that in the non-uniform angle distribution the populations of $\cos(\theta) = \pm 1.0$ (angles of 0° and 180°) are one third to one fourth of those at the maximum. Thus, parallel and anti-parallel orientations of the dipoles with $\vec{r}$ are frequently encountered and with a moderately higher frequency of the anti-parallel orientation at a certain dr interval. The same features as for 300 K are also observed at temperature 350 K, however at 350 K the distribution is broader (as shown in Figs. S5 and S4). At $T = 350$ K the shift from negative to positive $\cos(\theta)$ values is also observed as one moves from the inner to the outer solvent shells. Our results are consistent with those of Zakharov et al.[S1,S2] regarding the negative shift of the $\cos(\theta)$ distribution that we find in the inner water layers. Zakharov et al.[S1,S2] find a 90° angle in the outer layers. In the range 35.0 Å$< r <$37.0 Å, which is the red shell in Fig. S2 (b), we find that the $\cos(\theta)$ distribution is symmetric with respect to 0.0 as shown in Fig. S4 (e). This distribution leads to $\langle \cos(\theta) \rangle = 0$ (where $\langle \cdots \rangle$ denotes average). The $\cos(\theta)$ distribution has its maximum at 0.0 (which corresponds to 90°) but the majority of the dipoles deviate from the 90° angle. The red shell is characterized by roughness, thus the 90° angle is not on a smooth surface. In the farthest outer layers, where the density is very low, we see a positive shift in the $\cos(\theta)$ distribution.

Figure S6 shows the $\langle\cos(\theta)\rangle$ as a function of r for the pristine and charged droplets at $T = 300$ K. Figure S6 complements Fig. 4 (b) in the main text. The collection of plots for neutral and charged droplets allows for a direct comparison. Fig. S6 (a) shows that the surrounding vapor is polarized around the charge droplet and that the density of charged droplet surface is higher than that of the neutral. Fig. S6 (b) shows that in longer distance from the droplet COM the density of the vapor surrounding the neutral droplet is constant but that of the charged droplet decays. The vapor distribution around the droplet is determined by the electric field in the exterior of the droplet.

The overall picture that arises from our simulations is that at $r = 33.0 \pm 0.5$ Å, which is before a considerable decrease in the water density takes place, there is a negative shift in the $\cos(\theta)$ distribution. In the range of 35.0 Å$< r <$37.0 Å, which is the region of rough surface with low density, the $\cos(\theta)$ distribution is symmetric with respect to zero, thus, $\langle\cos(\theta)\rangle = 0$. In this shell, the majority of dipoles have an angle close to 90°, with equal probability of positive and negative deviations from the 90°.

Now, we discuss details about the angle distribution of the 1000 TIP3P H_2O-molecule droplet at $T = 300$ K and $T = 350$ K. Firstly, the distribution at $T = 300$ K is discussed. At $r <$ 13.0 Å the distribution of the $\cos(\theta)$ values is uniform, thus there is no preferred direction in the orientation of the dipoles. At 13 Å $< r <$ 19 Å the $\cos(\theta)$ distribution is an inverted parabola, with a flat maximum in the $\cos(\theta)$ range $-0.25 - 0$. Within this range, at 15.5 Å $< r <$ 17.5 Å the population of the oxygen sites is the highest as it is also shown in Fig. S1. At $r >$ 17.5 Å the oxygen population decays, which indicates that the density of the droplet decreases considerably. At 16.0 Å $< r <$17.5 Å the highest population of $\cos(\theta)$ is in the range $-0.5 - 0.3$, which corresponds to angles $120° - 72.5°$. At 19 Å $< r <$ 20 Å the $\cos(\theta)$ distribution in almost (with a marginal negative $\cos(\theta)$ shift) symmetric with respect to zero. At $r >$ 20 Å the $\cos(\theta)$ distribution shows a broad maximum in the range of $0 - 0.25$. At $r >$ 21.0 Å, the $\cos(\theta)$ distribution decreases by an order of magnitude than that in the range of 16.0 Å $< r <$ 17.5 Å. It is noted that in the non-uniform angle

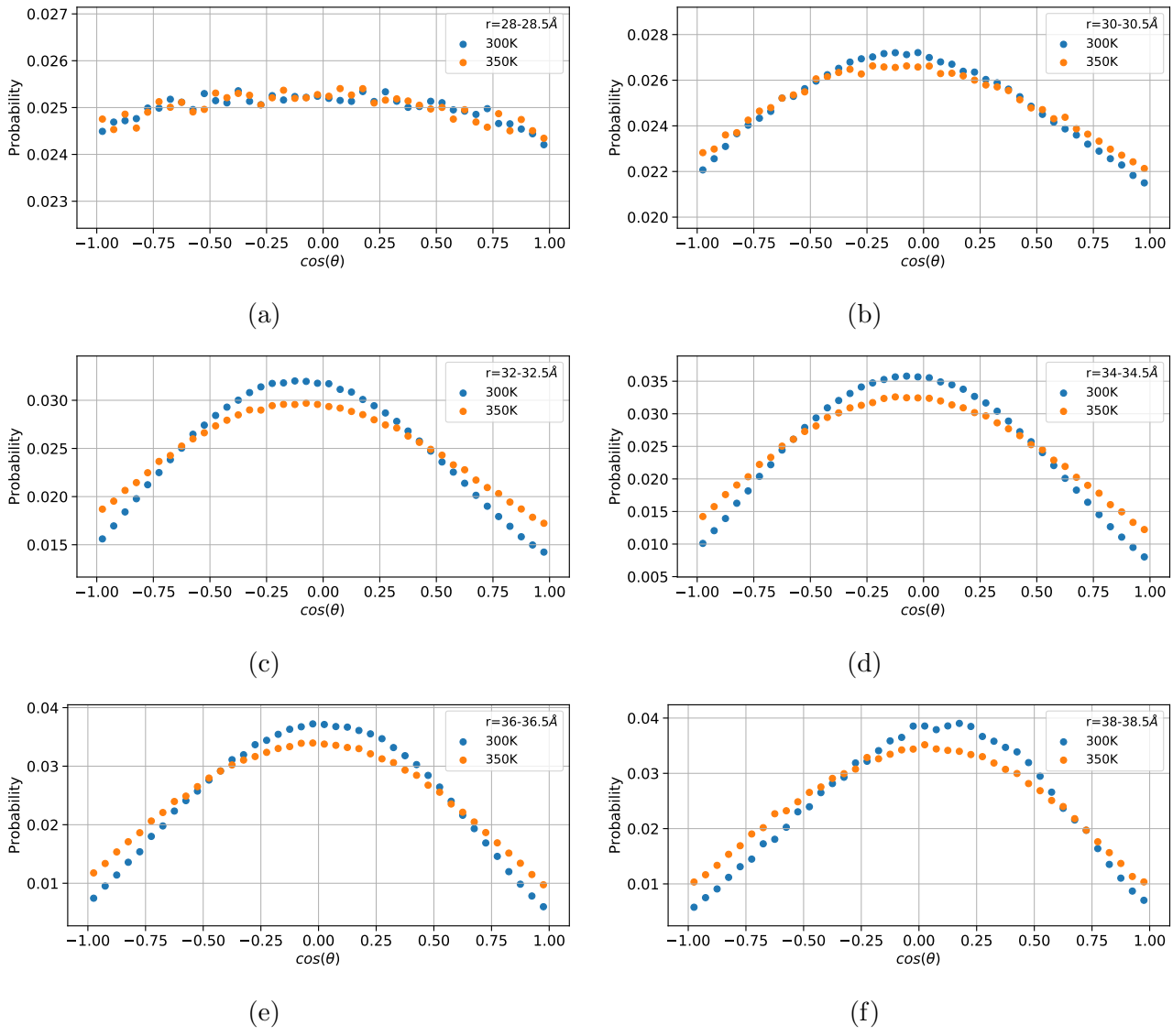

Figure S4: Probability of $\cos(\theta)$ at representative spherical shells around the droplet center of mass (COM) for pristine droplets comprised ≈ 6000 TIP3P H_2O molecules at $T = 300$ K and $T = 350$ K.

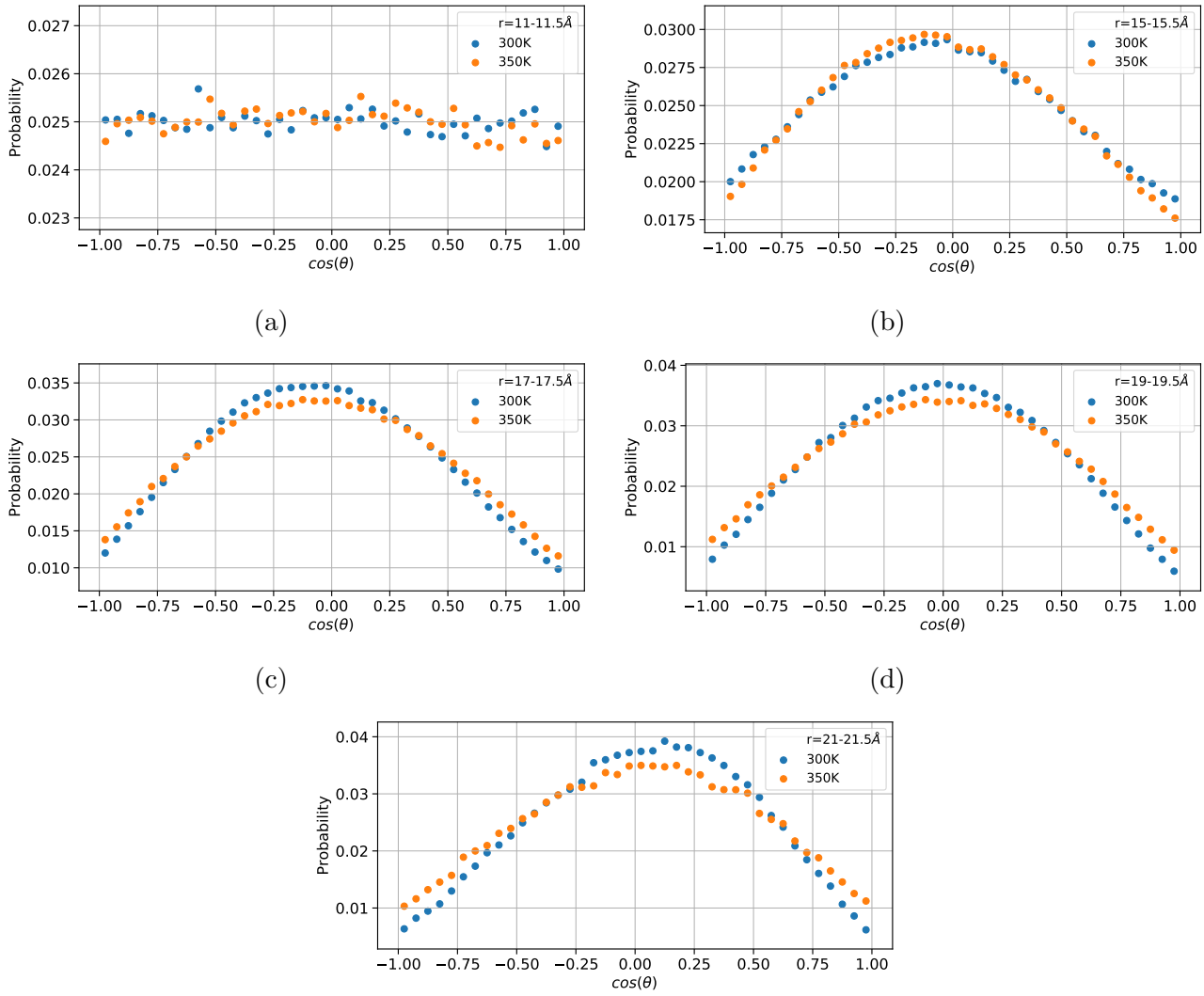

Figure S5: Same as Fig. S4 but for $\approx$ 1000 TIP3P H_2O molecules at $T = 300$ K and $T = 350$ K.

distribution the population of $\cos(\theta) = \pm 1.0$ (angles of 0° and 180°) are one third to one fourth of those at the maximum. Thus, parallel and anti-parallel orientations of the dipoles with $\vec{r}$ are frequently encountered and with a modestly higher frequency of the anti-parallel orientation at a certain dr interval. The same features as for $T = 300$ K are also observed at temperature 350 K, however at 350 K the distribution is broader. The shift toward negative and positive $\cos(\theta)$ values is also observed from the inner to the outer solvent shells. The overall picture is that at $r = 17.5 \pm 0.5$ Å, which is at a distance before a considerable decrease in the density takes place, there is a negative shift in the $\cos(\theta)$ distribution. In the regions where the density of the droplet is very low there is a positive shift.

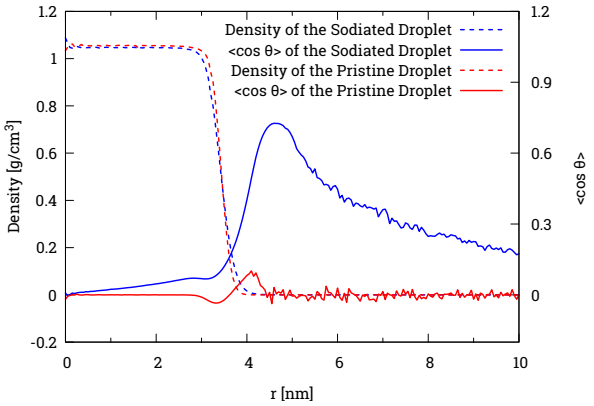

(a)

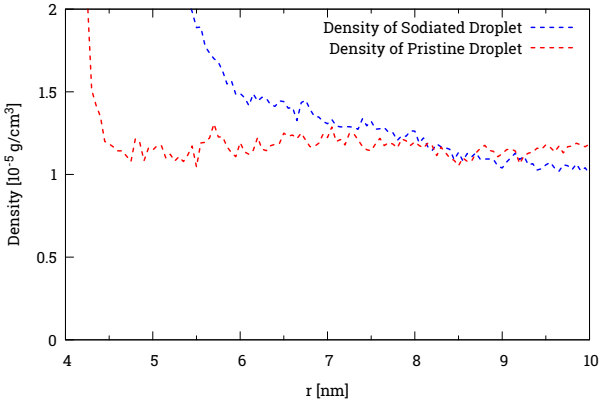

(b)

Figure S6: (a) $\langle\cos(\theta)\rangle$ as a function of r for a pristine and sodiated 6000-TIP3P droplet and vapor in the cavity at $T = 300$ K. The density profiles of water are shown. (b) Magnification of the TIP3P density decay at $r > 4$ nm of (a).

Ion spatial distribution in aqueous droplets

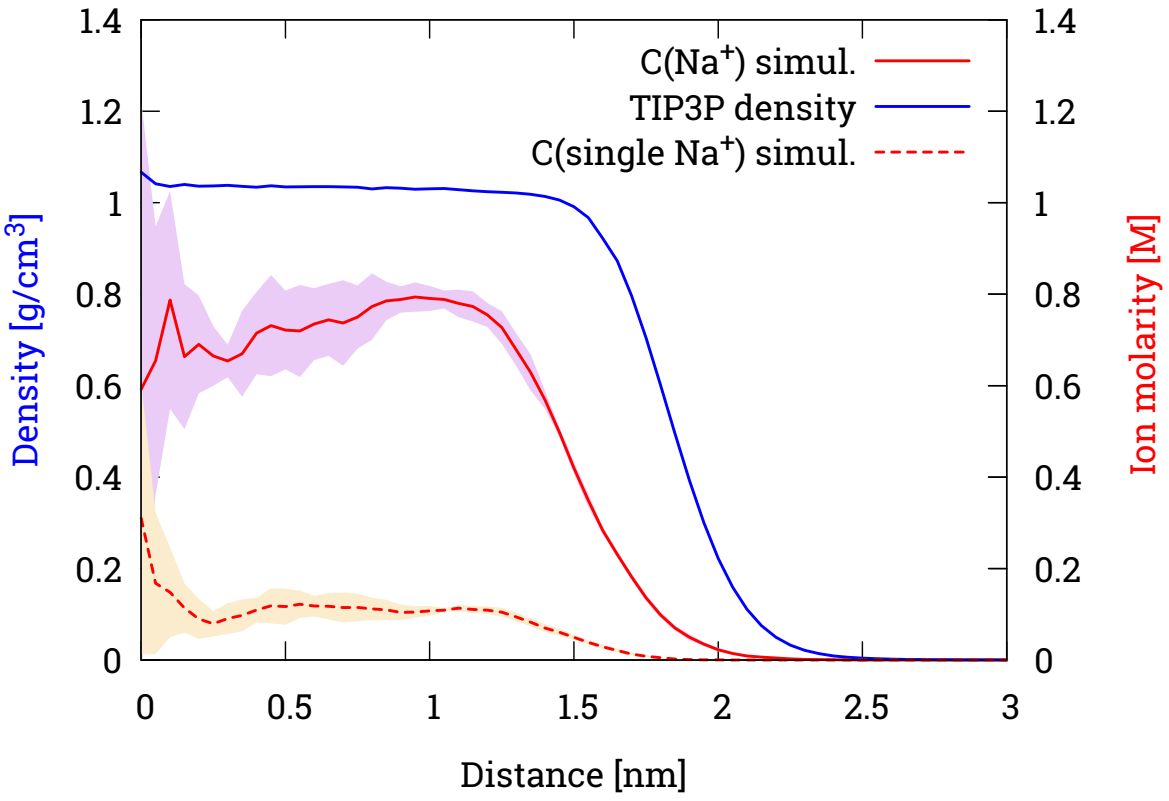

Figure S7: Water density (blue line) and ion concentration of a droplet comprised 880 water molecules, and 6 Na^+ ions (solid red line) and that of a droplet comprised 880 water molecules and a single Na^+ (dashed red line) at $T = 350$ K. The blurry regions delimits the error bars (one standard deviation).

Figure S7 shows the Na^+-CP of droplets that comprise 880 water (TIP3P) molecules and (a) 6 Na^+ ions and (b) a single Na^+ ion. The simulations show that the concentration of a single Na^+ is higher in the interior ($r < 1.5$ nm) of the droplet and decays towards its surface. The location of the single Na^+ ion is consistent with previous studies in smaller clusters.[S15–S19] Electrostatic theory, which is based solely on the energetic factor, predicts that a point charge will be located at the center of a dielectric medium with higher dielectric constant than the surrounding medium.[S20] Simple ions are not point charges, thus, the predictions of electrostatic theory is not always sufficient to determine the ion location. Factors such as the ion size and ion-solvent charge transfer may play a role in determining

their location in a droplet. In the particular system that we study the simulations show a broad single Na^+-CP in the droplet interior, which arises because of the thermal motion of the droplet constituents (entropic factor). Thus, the location of the single Na^+ follows the predictions of electrostatics on the fact that the ion is located in the droplet interior, but as expected, the Na^+-CP is broad because of thermal motion.

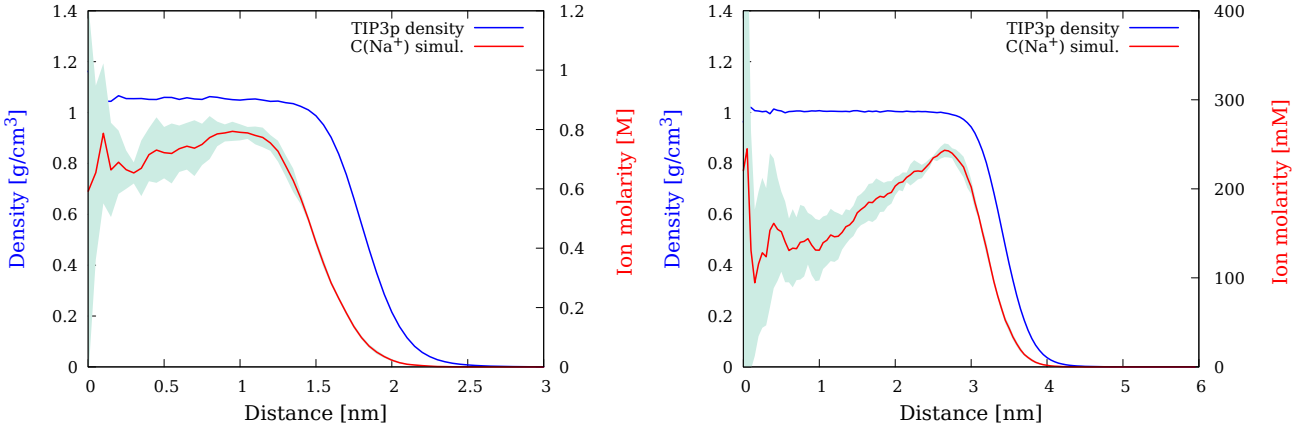

Figure S8: Distributions of Na^+ ions (red line) and oxygen sites (blue line) in droplets comprised (a) 980 TIP3P molecules and 8 Na^+ ions at $T = 300$ K. and (b) 5990 TIP3P molecules and 18 Na^+ ions at $T = 350$ K. The error bars are shown by the light green region.

Figure S8 (a) shows the DP of the oxygen (O) sites of H_2O molecules and the concentration profile (CP) of Na^+ ions for a droplet comprised ≈ 1000 H_2O molecules and 8 Na^+ ions at $T = 300$ K. The H-DP and O-DP are very close to each other at both temperatures. The H-DP raises over the O-DP at 18.15 Å . At $T = 300$ K the Na^+-CP (red line in Fig. S8 (a)) shows a pronounced broad distribution in the range of 4.5 Å − 12.5 Å, which has a flat maximum in the range of 8.4 Å − 11.0 Å. In $r < 3.2$ $\mathring{A}$ there is still a non-negligible ion density, which does not become zero even at the center of the droplet. The error bars were estimated by using 5 blocks of 10^5 configurations each. In the range of 0 $\mathring{A} \leq r < 3.2$ $\mathring{A}$ the Na^+-CP error bars are larger due to poorer statistics.

Figure S9 compares the spatial extent of an $\approx$ 6000-H_2O molecule droplet with and without Na^+ ions at $T = 300$ K and $T = 350$ K. At both temperatures the DP of the

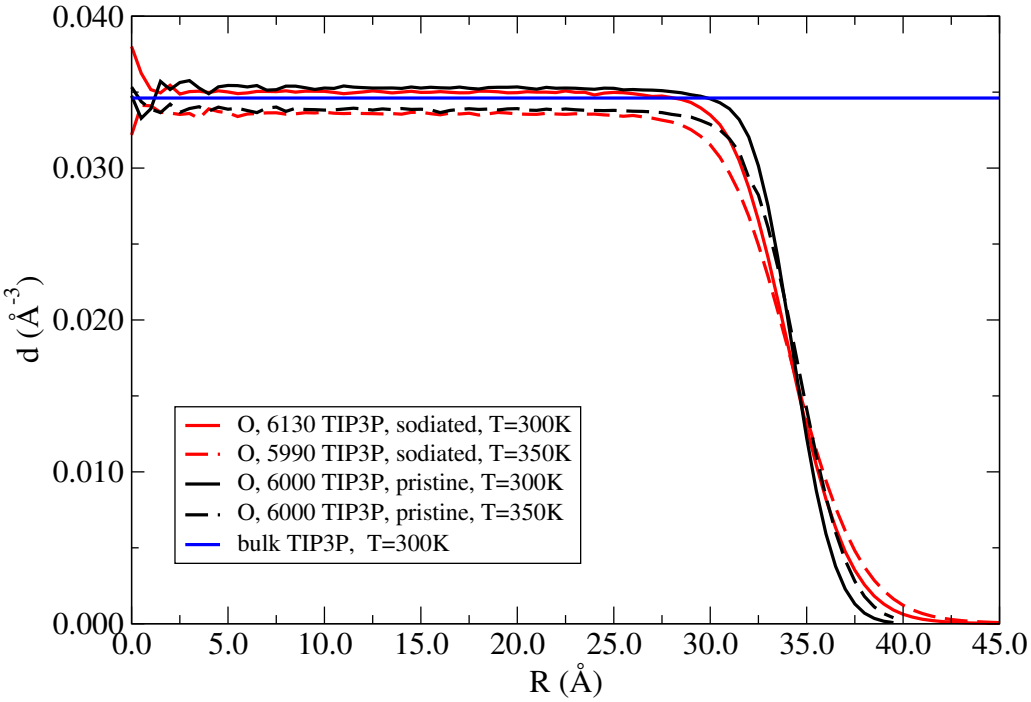

Figure S9: Comparison between the oxygen-DPs of droplets comprised $\approx$ 6000 H_2O molecules and 20 Na^+ ions (red lines) and pristine aqueous droplets of $\approx$6000 molecules (black lines) at $T = 300$ K and 350 K.

pristine aqueous droplet dies-off faster than that of the charged droplet. We may attribute the difference in size primarily to the different shape fluctuations of the charged droplet from that of the pristine droplet. The larger size of the charged droplet may also be affected to a lesser degree by the additional volume of the Na^+ ions and the larger number of H_2O molecules that remain bound in the charged droplet relative to the pristine droplet under equilibrium conditions.

Angle distribution of sodiated aqueous droplets

In more detail the $\cos(\theta)$ distribution shown in Fig. 4 (a) in the main text is as follows: In a spherical shell of r =2.5 Å the $\cos(\theta)$ distribution averages to zero and is uniform for both droplet sizes. At r >2.5 Å there is a gradual shift toward the positive $\cos(\theta)$ values. At $r = 10 \pm 0.5$ Å there is a moderate shift toward positive $\cos(\theta)$ values especially in the range of $0.45 - 1$. At $r = 15 \pm 0.5$ Å there is a moderate shift toward positive $\cos(\theta)$ values in the range of $0.80 - 1$ (20% higher population with $\cos(\theta)$ +1 than −1). Now, we shall examine the features of the angle distribution at 17.0 Å $< r <$ 28.5 Å, which is the interval where the probability density of Na^+ ions is the highest. At $r = 17.0 \pm 0.5$ Å even though all the angles are substantially populated, the higher $\cos(\theta)$ values are increasingly populated and the maximum is at $\cos(\theta) = +1$. The population of H_2O molecules with $\cos(\theta) = +1$ are ≈ 20% more than those with $\cos(\theta) = -1$. At 25.0 Å $< r <$ 26.0 Å the increase of the population of the positive $\cos(\theta)$ values in the range $0.75 - 1.0$ (40% higher $\cos(\theta) = +1$ population than −1) becomes more pronounced. At $r = 28.5 \pm 0.5$ Å the $\cos(\theta)$ distribution is strongly shifted toward the positive values where a broad range of angles with $\cos(\theta)$ values $0.5 - 1.0$ (which corresponds to angle range $60° - 0°$) are highly populated. The $\cos(\theta) = 1$ has a marginal maximum population. For 29.0 Å $< r <$ 39.0 Å $\cos(\theta) = 1$ is highly populated but it is not the maximum as in the smaller r. The maximum $\cos(\theta)$ value shifts gradually toward the range of $0.25 - 1.0$ at $r = 29 \pm 0.5$ Å, to $0.0 - 1.0$ (almost uniform distribution) at $r = 30 \pm 0.5$ Å, to $0.0 - 0.50$ at 32 Å$< r <$ 34 Å. Close to $r = 34$ Å the angles are in the range of $66° - 90°$ with the maximum found at 75° ($\cos(\theta)$) = 0.25). At 37.0 Å $< r <$ 38.0 Å the highest $\cos(\theta)$ population is in the range $0.25 - 1.0$, which shows an almost uniform distribution. For $r \approx 39.0$ Å there is a strong preference for larger $\cos(\theta)$) values in the range of $0.50 - 1.0$. The population is approximately 50% more for the droplet at $T = 350$ K than at $T = 300$ K. We attribute this difference to the fact that the lower temperature droplet is less extended than the higher temperature one. For $r \geq 40.0$ Å, where the dipole population is minimal, there is a clear preference for $\cos(\theta) = 1.0$. These

water molecules are far away so as they view the rest of the droplet as a central charge. At this distance the conducting or dielectric character of the droplet does not play a role.[S21]

A typical snapshot of a droplet comprised $\approx$ 1000 TIP3P molecules and 8 Na^+ ions is shown in Fig. S10.

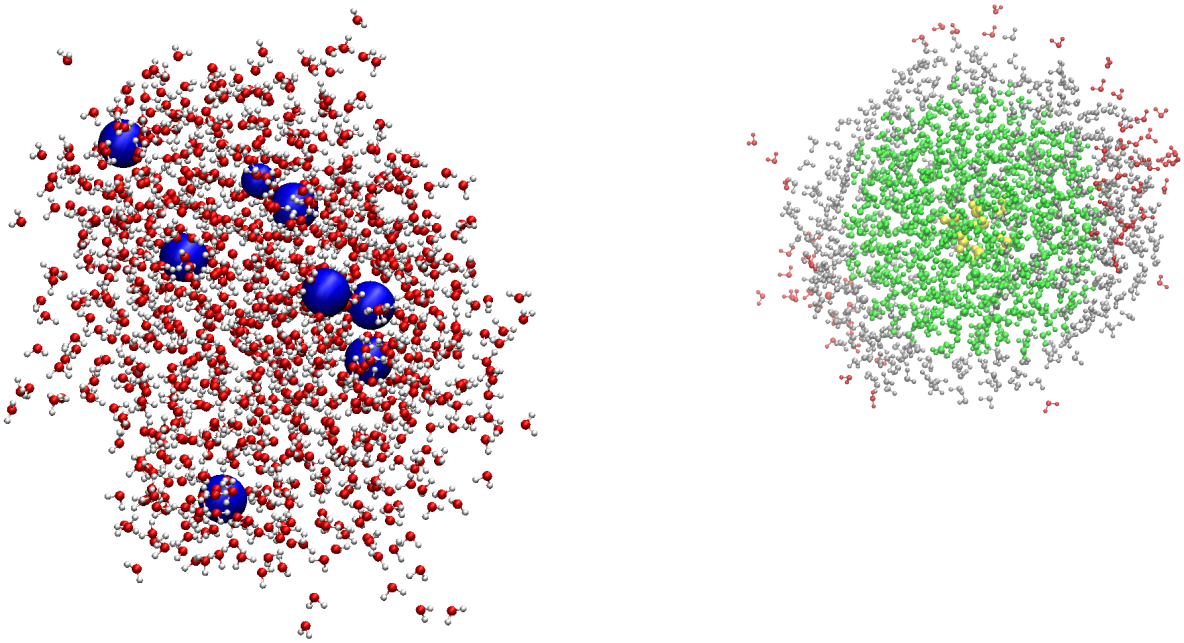

(a) (b)

Figure S10: (a) Typical snapshot of a droplet comprised $\approx$ 1000 TIP3P molecules and 8 Na^+ ions. The Na^+ ions are shown by the blue spheres and the oxygen sites by the red colored spheres. (b) Colored shells around the droplet COM at various r (the Na^+ ions are not shown): yellow colored 0 Å $< r <$ 3.2 Å, green colored 3.2 Å $< r <$ 15.0 Å, grey colored 15.0 Å $< r <$ 21.0 Å, red colored $r >$ 21.0 Å.

Figure S11 is a typical snapshot of an enlarged region of the droplet that shows magnified the water molecules in a radius of 4.0 Å from a Na^+. Even though this is a typical snapshot the orientation of the H_2O dipoles is affected by the location of the Na^+ in the droplet, surface vs. interior. The orientation of the H_2O dipole even in the first solvation shell is subject to thermal fluctuations.

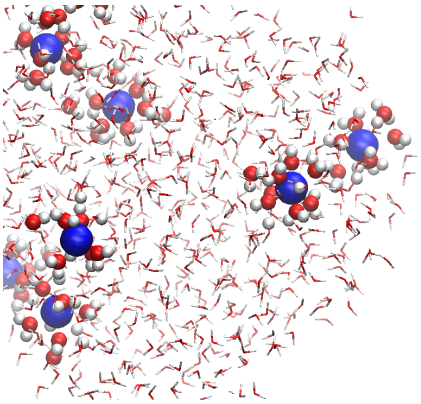

Figure S11: A typical snapshot, magnifying a region of a droplet, to show the orientation of the water molecules around a Na^+ ion. The droplet is comprised $\approx$ 1000 TIP3P molecules and 8 Na^+ ions at $T = 300$ K.

Here, we discuss the angle distribution of $\approx$ 1000 TIP3P H_2O molecules and 8-6 Na^+ ions at $T = 300$ K and $T = 350$ K as shown in Fig. S12. At 7.5 Å$\leq r \leq$ 13.0 Å, which includes the highest probability density for Na^+ ions to be encountered, the $\cos(\theta)$ range $0.60 - 1.0$ (angles range: $53° - 0°$) shows a considerable population with maximum at $\cos(\theta) = 1.0$. The $\cos(\theta)$ distribution is more uniform at $T = 350$ K. At $r = 15.0 \pm 0.5$ Å the distribution is shifted toward positive $\cos(\theta)$ values. The maximum of the distribution is in the $\cos(\theta)$ range $0.25 - 0.5$ (angle range: $75° - 60°$). The $\cos(\theta)$ value 0.95 ± 0.05 (angle of $0°$) is highly populated but is in not the maximum. At 15.5 Å $\leq r \leq$ 17.0 Å the $\cos(\theta)$ distribution is clearly shifted toward the positive values in the range of $0.0 - 0.50$ (angle range: $90° - 60°$). At $r = 19 \pm 0.5$ Å the maximum is in the $\cos(\theta)$ range $0.25 - 0.60$ (angle range: $75° - 53°$). At 21 Å $\leq r \leq$ 23 Å there is almost a linear increase in the $\cos(\theta)$ population from -1 to $+1$. At this range the population of the oxygen sites has decreased significantly relative to smaller r, which indicates that the density of the water molecules has decreased relative to smaller r. For $r >$ 27.5 Å the number of counts becomes negligible. At $T = 350$ K the features of the $\cos(\theta)$ distribution are the same as for $T = 300$ K but the distributions are broader as expected due to the thermal motion. The picture that emerges from the $\cos(\theta)$ distribution is that in the r distance where the Na^+-CP shows the high probability the angles do not show maximum at $0°$ but they explore a range of $0° - 90°$. A broad distribution of

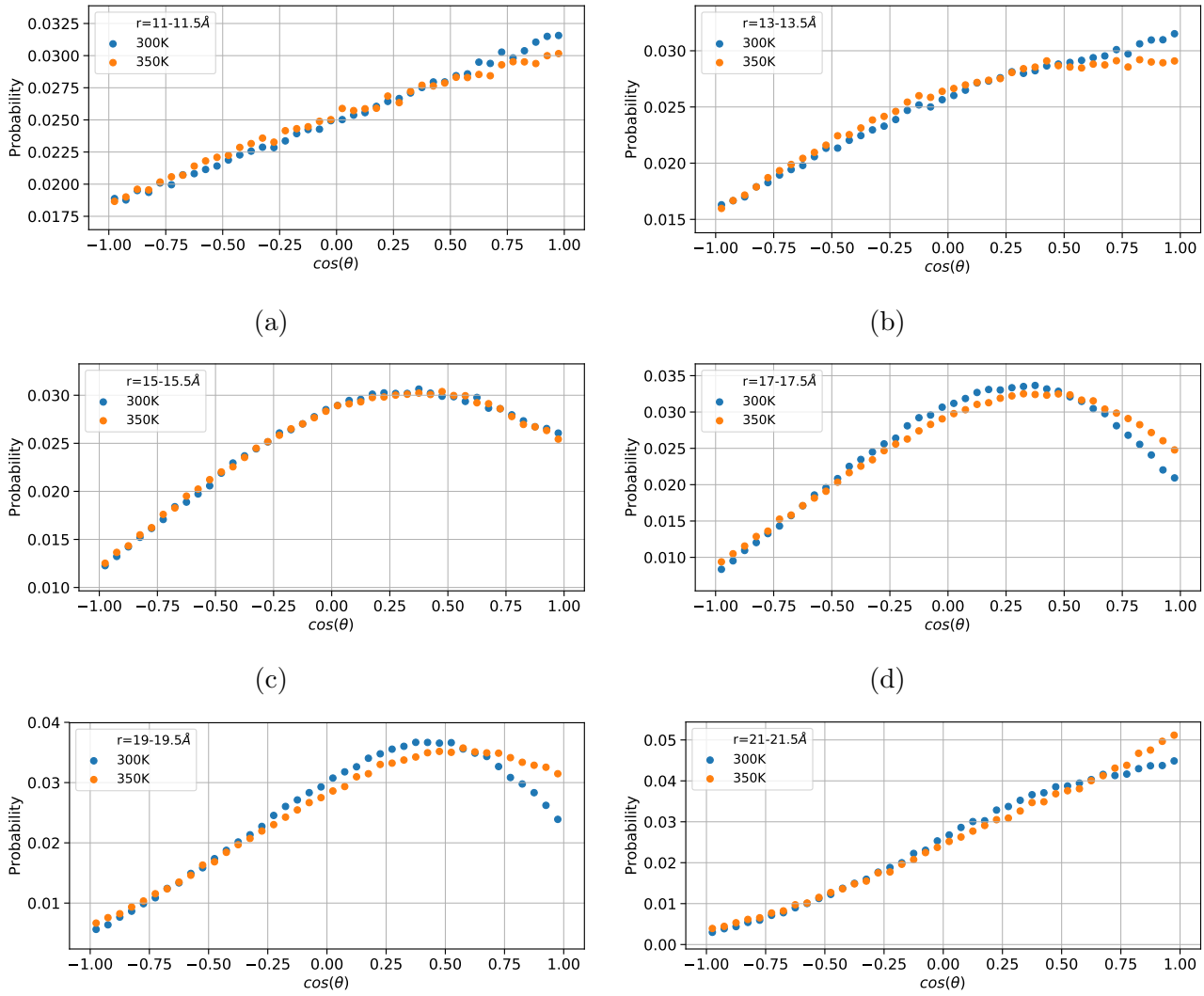

Figure S12: Same as Fig. S5 but for ≈ 1000 TIP3P H_2O molecules and 8-6 Na^+ ions at $T = 300$ K and $T = 350$ K.

angles is to be expected because as the H_2O molecules are polarized around every Na^+, their orientation varies. Considering bulk simulations, it is expected that the solvent orientation will be strongly affected by the Na^+ over two coordination shells. At $r > 23$ Å the H_2O molecules are strongly oriented by the electrostatic field of the entire droplet and not the individual Na^+ ions. Thus, the water dipole moment and $\vec{r}$ are at 0° angle. The observation of the strong orientation shows that the strength of the electric field overcomes the thermal motion.

Charge distribution

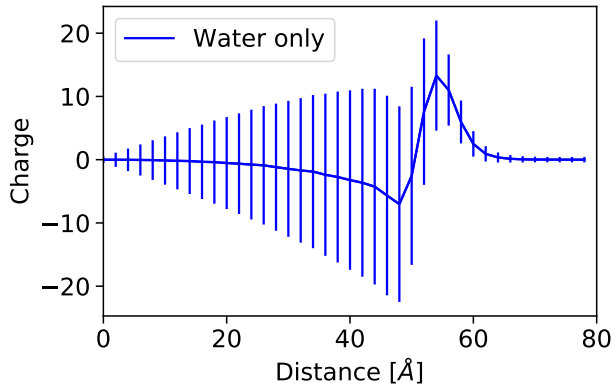

(a)

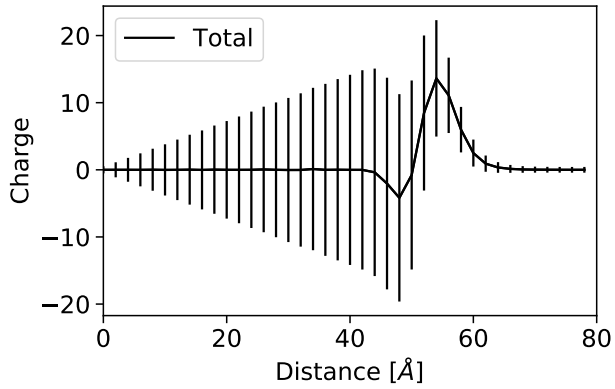

(b)

Figure S13: Charge distribution in a droplet comprised 2×10^4 water molecules and $36\mathrm{Na}^+$ ions at $T = 350\mathrm{K}$. The distribution is calculated by finding the charge in spherical shells centered at the droplet COM. (a) Water only. (b) Water and ions.

The fluctuations in the charge distribution are shown in Fig. S13 for a droplet comprised 2×10^4 water molecules and $36\mathrm{Na}^+$ ions at $T = 350\mathrm{K}$.

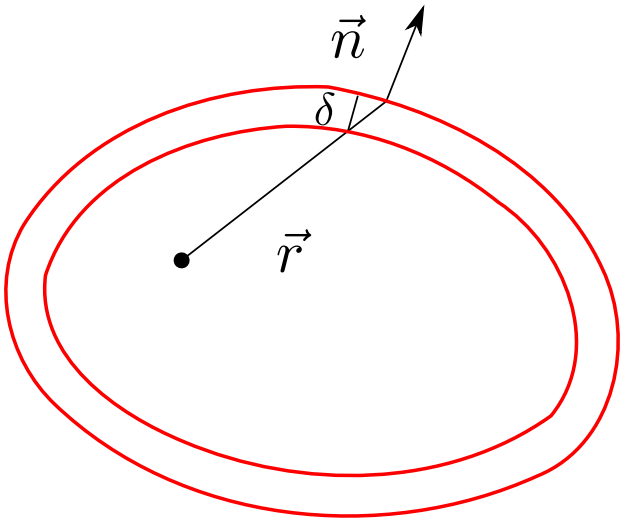

Figure S14: Illustration of the change in the radius vector when the surface is offset by a fixed distance δ.

Orientation of water molecules in sodiated droplets with polyhistidine

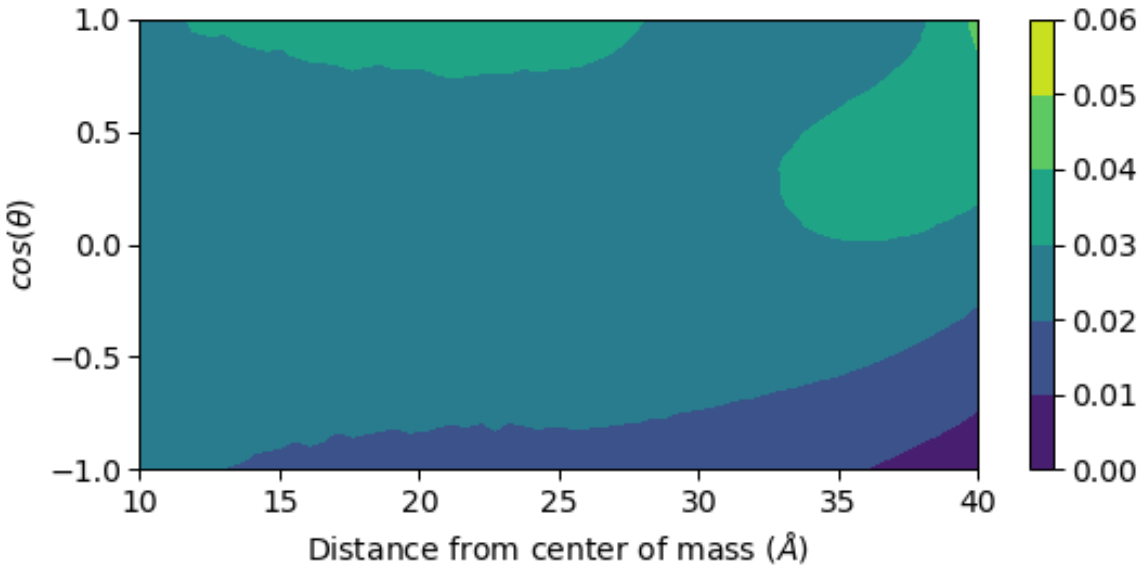

Figure S15: Same as Fig.S3 but for a droplet composed of 6000 H_2O molecules, His_{10}^{10+}, and 10 Na^+ ions (3 have evaporated) at T = 350K. For the histograms, 50000 configurations collected every 0.2 ps and a bin size is 0.5 Å were used.

At $T = 350$ K the general features of the angle distribution are consistent to those found at $T = 300$ K. The description of the distribution is as follows: at $r < 14.0$ Å all angles are well populated. At $r = 14.0 \pm 0.5$ Å there is an $\approx 5\%$ shift of the population toward the positive $\cos(\theta)$ values, with the maximum found at $\cos(\theta) = +1$. At $r = 16.0 - 17.0$ Å there is a broad almost uniform population in the $\cos(\theta)$ range $0.55 - 1$, with a marginal maximum at $\cos(\theta) = +1$. At $r = 19.0 - 27.5$ Å there is a broad almost uniform distribution in the $\cos(\theta)$ range $0.80 - 1$. The value of $\cos(\theta) = +1$ is clearly the maximum at $r = 22.0 - 25.0$ Å. For $r \geq 29.0$ Å there is a gradual shift of the population toward $\cos(\theta) = 0$. At $r = 30.0$ Å the $\cos(\theta)$ range $0.1 - 0.75$ is highly populated. The $\cos(\theta) = 0.0$ has a comparable population to the positive $\cos(\theta)$. At $r > 30$ Å the population of low negative $\cos(\theta)$ values becomes comparable to the positive $\cos(\theta)$ values.

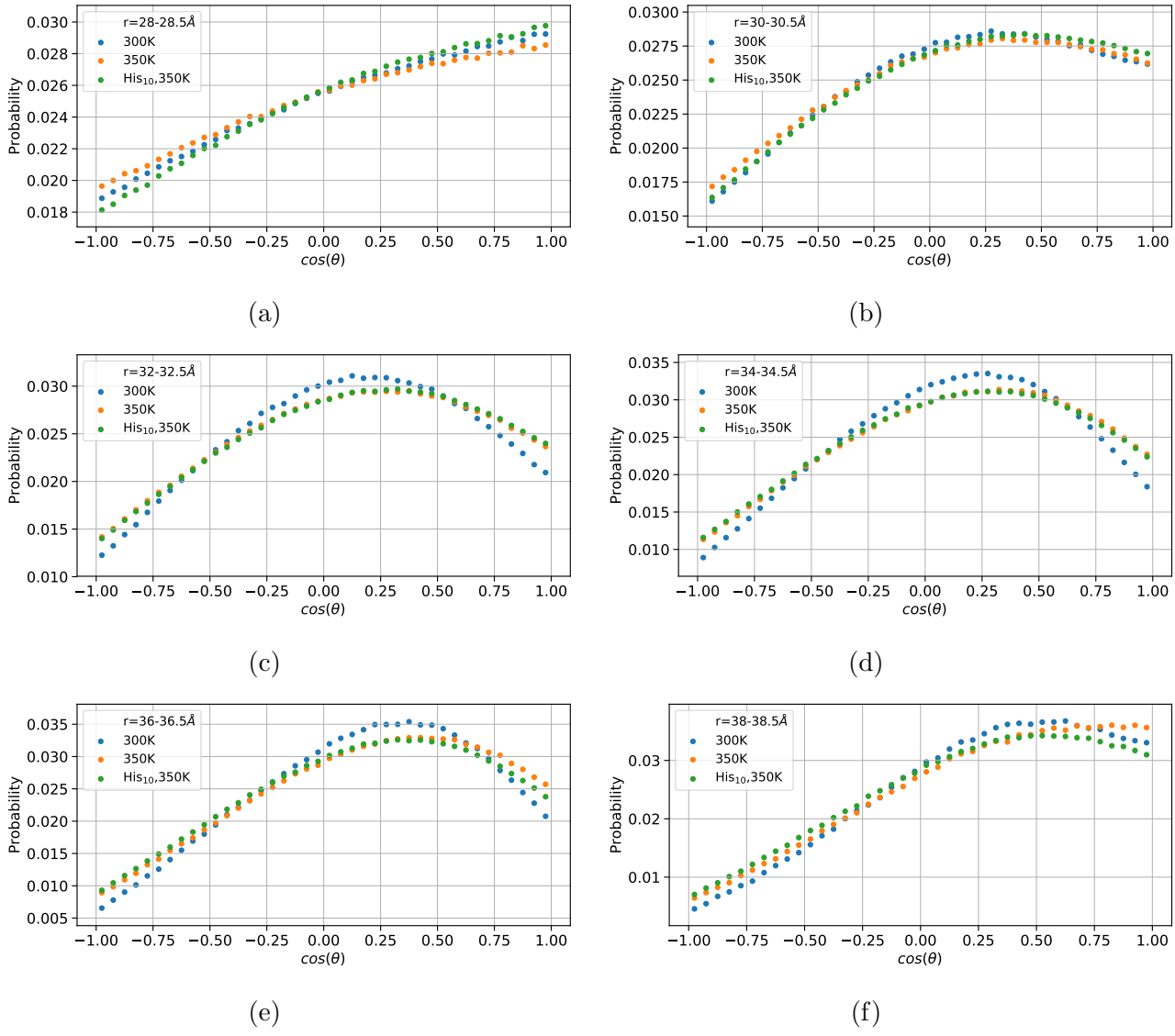

Figure S16: Same as Fig. S5 but for droplets of $\approx$ 6000 TIP3P H_2O molecules with 20 Na^+ ions at $T = 300$ K and $T = 350$ K (blue and orange colored dots) and $\approx$ 6000 TIP3P H_2O molecules, 10 Na^+ ions and a His_{10}^{10+} (green dots).

References

(S1) Zakharov, V. V.; Brodskaya, E. N.; Laaksonen, A. Surface properties of water clusters: a molecular dynamics study. *Mol. Phys.* **1998**, *95*, 203–209.

(S2) Zakharov, V. V.; Brodskaya, E. N.; Laaksonen, A. Surface tension of water droplets: A molecular dynamics study of model and size dependencies. *J. Chem. Phys.* **1997**, *107*, 10675–10683.

(S3) Jorgensen, W. L.; Jenson, C. Temperature dependence of TIP3P, SPC, and TIP4P water from NPT Monte Carlo simulations: Seeking temperatures of maximum density. *J. Comput. Chem.* **1998**, *19*, 1179–1186.

(S4) Mahoney, M. W.; Jorgensen, W. L. A five-site model for liquid water and the reproduction of the density anomaly by rigid, nonpolarizable potential functions. *J. Chem. Phys.* **2000**, *112*, 8910–8922.

(S5) Mark, P.; Nilsson, L. Structure and dynamics of the TIP3P, SPC, and SPC/E water models at 298 K. *J. Phys. Chem. A* **2001**, *105*, 9954–9960.

(S6) Tolman, R. C. The effect of droplet size on surface tension. *J. Chem. Phys.* **1949**, *17*, 333–337.

(S7) Homman, A.-A.; Bourasseau, E.; Stoltz, G.; Malfreyt, P.; Strafella, L.; Ghoufi, A. Surface tension of spherical drops from surface of tension. *J. Chem. Phys.* **2014**, *140*, 034110.

(S8) Block, B. J.; Das, S. K.; Oettel, M.; Virnau, P.; Binder, K. Curvature dependence of surface free energy of liquid drops and bubbles: A simulation study. *J. Chem. Phys.* **2010**, *133*, 154702.

(S9) Rowlinson, J. A drop of liquid. *J. Phys.: Condens. Matter* **1994**, *6*, A1.

(S10) Horsch, M.; Hasse, H.; Shchekin, A. K.; Agarwal, A.; Eckelsbach, S.; Vrabec, J.; Müller, E. A.; Jackson, G. Excess equimolar radius of liquid drops. *Phys. Rev. E* **2012**, *85*, 031605.

(S11) Malijevskỳ, A.; Jackson, G. A perspective on the interfacial properties of nanoscopic liquid drops. *J. Phys.: Condens. Matter* **2012**, *24*, 464121.

(S12) G Segovia-López, J.; Carbajal-Domínguez, A. Pressure tensor of nanoscopic liquid drops. *Entropy* **2015**, *17*, 1916–1935.

(S13) Tröster, A.; Oettel, M.; Block, B.; Virnau, P.; Binder, K. Numerical approaches to determine the interface tension of curved interfaces from free energy calculations. *J. Chem. Phys.* **2012**, *136*, 064709.

(S14) Vega, C.; de Miguel, E. Surface tension of the most popular models of water by using the test-area simulation method. *J. Chem. Phys.* **2007**, *126*, 154707.

(S15) Perera, L.; Berkowitz, M. L. Many-body effects in molecular dynamics simulations of Na+ (H2O) n and Cl-(H2O) n clusters. *J. Chem. Phys.* **1991**, *95*, 1954–1963.

(S16) Asthagiri, D.; Pratt, L. R.; Ashbaugh, H. Absolute hydration free energies of ions, ion–water clusters, and quasichemical theory. *J. Chem. Phys.* **2003**, *119*, 2702–2708.

(S17) Hagberg, D.; Brdarski, S.; Karlström, G. On the solvation of ions in small water droplets. *J. Phys. Chem. B* **2005**, *109*, 4111–4117.

(S18) Stuart, S. J.; Berne, B. Surface curvature effects in the aqueous ionic solvation of the chloride ion. *J. Phys. Chem. A* **1999**, *103*, 10300–10307.

(S19) Caleman, C.; Hub, J. S.; van Maaren, P. J.; van der Spoel, D. Atomistic simulation of ion solvation in water explains surface preference of halides. *Proc. Natl. Acad. Sci. U.S.A.* **2011**, *108*, 6838–6842.

(S20) Jackson, J. D. *Classical Electrodynamics*, 3rd ed.; John Wiley & Sons: New York, NY, 1998.

(S21) Consta, S. Manifestation of Rayleigh instability in droplets containing multiply charged macroions. *J. Phys. Chem. B* **2010**, *114*, 5263–5268.